Chapter 4
Collective Excitations in Supercritical Fluids

Taras Bryk, Federico Gorelli, Giancarlo Ruocco, Mario Santoro and Tullio Scopigno

Abstract Recent progress in theoretical and simulation studies of collective excitations in supercritical fluids is reviewed. We discuss a methodology of fit-free estimation of dispersion of longitudinal and transverse excitations in simple fluids. The issue of vanishing positive sound dispersion—a viscoelastic increase of the speed of sound from adiabatic one to its high-frequency (elastic) value—with reduction of density, as it was observed in inelastic X-ray scattering experiments on supercritical Ar, is discussed from the point of view of finding distinctions in collective dynamics of low—and high-density supercritical fluids. On the basis of several theoretical models within the extended hydrodynamic description of density-density correlations in liquids analytical expressions for positive sound dispersion are obtained and applied for analysis of time correlation functions obtained from molecular dynamics simulations. A location of a crossover from the liquid-like to gas-like types of collective dynamics is discussed based on general findings for spectra of collective excitations in supercritical Ar and soft sphere fluids.

T. Bryk (✉)
Institute for Condensed Matter Physics of the National Academy of Sciences of Ukraine, 1, Svientsitskii Street, Lviv 79011, Ukraine
e-mail: bryk@icmp.lviv.ua

F. Gorelli · M. Santoro
Istituto Nazionale di Ottica, CNR-INO, and LENS, 50019 Sesto Fiorentino, Italy

G. Ruocco · T. Scopigno
Dipartimento di Fisica, Universita di Roma La Sapienza, 00185 Rome, Italy

G. Ruocco
Center for Life Nano Science @Sapienza, Istituto Italiano di Tecnologia, 295 Viale Regina Elena, 00161 Rome, Italy

L. Bulavin and N. Lebovka (eds.), *Physics of Liquid Matter: Modern Problems*, Springer Proceedings in Physics 171, DOI 10.1007/978-3-319-20875-6_4

4.1 Introduction

Collective excitations in disordered systems being one of the most sophisticated and fascinating problems of modern condensed matter physics attracted focus of many theoretical, experimental and simulation groups. An interplay of different spatial and temporal scales makes the probes of collective excitations in liquids and glasses by scattering experiments and computer simulations very important for unveiling details of their dispersion at different thermodynamic conditions. In particular, the change in collective dynamics of fluids above the liquid-gas critical point can reveal fundamental dissimilarities in collective behaviour of matter in different states—from a liquid-like type of dynamics for dense fluids to a gas-like one for rarified fluids.

In his Nobel lecture Johannes van der Waals told that "I conceived the idea that there is no essential difference between the gaseous and the liquid state of matter" [1]. Until recently the supercritical fluids have been considered as a unique state with intermediate properties of the liquid and gas phases. There exists a traditional point of view on liquid and gas as phases of the same symmetry, that implies these phases cannot be distinguished above the critical point where they do not coexist. Structural studies of supercritical fluids completely support this point of view. However, there are examples, like the liquid-glass transition when the structure of both liquid and glass phases is of the same symmetry while the dynamic properties and in particular the behaviour of density-density time-dependent correlations reveal fundamental difference connected with the non-ergodicity of the glass state [2]. According to [2] below the glass transition temperature the density-density time correlation functions have non-vanishing with time tail, which is a measure of the non-ergodicity of the system. This effect corresponds to the dynamical arrest of particles in contrast to the liquid state for which the density-density correlations decay with time to zero. This example of the dissimilarity of collective dynamics for liquids and glasses reflects a sensitivity of dynamic quantities to the states of matter and implies a possibility to find some dynamic dissimilarities in the collective dynamics of liquids and gases.

Recent inelastic X-ray scattering (IXS) experiments performed for supercritical Oxygen [3] and Argon [4, 5] and experimentally obtained dispersions of collective excitations in these supercritical fluids revealed a strong reduction of a typical for dense fluids viscoelastic effect known as positive sound dispersion (PSD) with the decrease of density of the fluids. The viscoelasticity of liquids [6] is manifested in their collective dynamics mainly via several effects: (i) existence of a deviation from the linear hydrodynamic dispersion law for acoustic excitations towards higher frequencies-PSD, (ii) emergence of the short-wavelength shear waves (SW) and (iii) a crossover between thermal and structural relaxations as the main contributions to the relaxing behaviour of density-density correlations in long- and short-wavelength regions. It is known that liquids do not sustain macroscopic shear and therefore macroscopic transverse sound waves cannot propagate in liquids [7], however on molecular length scales the microscopic elasticity of fluids can cause

emergence of the short-wavelength transverse collective excitations-SW, which however are quite overdamped. The dynamic features of fluids due to their viscoelasticity-PSD and SW-can be the candidates to find dissimilarities in liquid-like and gas-like types of dynamics in supercritical region.

On the theoretical side the description of collective excitations in fluids must account for different space and time scales in dynamics of the studied systems. On macroscopic scales the analytical results must recover hydrodynamic expressions [8–12] for collective modes. The hydrodynamic theory [7, 13, 14] being a collection of fundamental local conservation laws treats the fluid as continuum without any atomistic structure. Therefore any extension of hydrodynamic theory must account for dynamic processes occuring on molecular space and time scales. Namely the generalized hydrodynamic models [7, 14] should be applied for correct understanding the origin of the viscoelastic effects. It is important to stress that the theoretical description of collective dynamics in fluids will be performed for the weakly nonequilibrium states of fluids and all the fluctuations are quite small that allows to neglect non-linear hydrodynamic fluctuations.

The paper is organized as follows: in the next section we will discuss the extended models of collective dynamics of liquids which enable calculations of dispersion of collective excitations and description of the viscoelastic effects such as positive sound dispersion and shear waves. The third section gives information on the computer simulations for supercritical Ar and application of the developed theoretical schemes to analysis of time correlation functions obtained in molecular dynamics simulations. A crossover in collective dynamics of supercritical fluids is discussed in the fourth section, and the last section contains conclusions of this study.

4.2 Theoretical Models of Collective Dynamics in Fluids

4.2.1 Hydrodynamic Approach

Perhaps historically first analytical treatment of collective modes in liquids was performed by Landau and Placzek [15] who published (without any details—just mentioning that the hydrodynamic equations were used) a very short communication on their famous Landau-Placzek ratio for the integral intensities of the scattered light in liquids that reads

$$\frac{I_R}{2I_B} = \gamma - 1.$$

Here $\gamma = C_P/C_V$ is the ratio of specific heats at constant pressure and volume, I_R and I_B are the integral intensities of the Rayleigh and Brillouin peaks of dynamic structure factor $S(k, \omega)$ with k and ω being wave number and frequency, respectively. The Landau-Placzek ratio is applicable only for essentially small wave

numbers. The dynamic structure factor as a function of wave number and frequency contains all the information about the spectral distribution of the scattered light by fluid, and for essentially small wave numbers the $S(k,\omega)$, as it was observed in the light-scattering experiments, has a three-peak shape. The Rayleigh peak centered at zero frequency is due to thermal relaxation while two side (Brillouin) peaks of $S(k,\omega)$ at frequencies

$$\pm\omega_B(k) = \pm c_s k, \tag{4.1}$$

are coming from acoustic collective excitations that propagate with the adiabatic speed of sound

$$c_s = [\frac{\gamma}{\rho\kappa_T}]^{1/2},$$

where ρ is mass density and κ_T is isothermal compressibility. The Landau-Placzek ratio is a measure of the visibility of the Brillouin peaks in $S(k,\omega)$ for small wave numbers. Since the dynamic structure factor is connected with the density-density time correlation function $F_{nn}(k,t) = \langle n(k,t)n^*(k,t=0)\rangle$ via time-Fourier transformation

$$S(k,\omega) = \int_0^\infty F_{nn}(k,t)e^{-i\omega t}dt \tag{4.2}$$

the main focus in theoretical studies is on obtaining analytical expressions for the density-density time correlation functions. In the definition of $F_{nn}(k,t)$ the $n(k,t)$ denotes the spatial-Fourier component of fluctuations of number density.

Active theoretical studies of hydrodynamic collective modes and their contributions to the density-density time correlation functions for simple and binary fluids have been performed during the period 1960–1970s [8–12]. The hydrodynamic approach for collective excitations in simple one-component fluids consists in solving a system of three equations—continuity equation, longitudinal part of Navier-Stokes equation and balance equation for energy—in terms of dynamic eigenmode. These three equations represent balance equations for three conserved quantities: total number of particles, longitudinal component of total momentum and total energy. Within the linearized hydrodynamics the transverse component of total momentum is decoupled from the other equations—hence, transverse collective modes in the long-wavelength can be treated separately. For transverse dynamics there exists only one balance equation for conserved quantity, which is the transverse component of total momentum.

According to [9] three balance equations for the longitudinal dynamics in hydrodynamic treatment can be represented in the Laplace-transformed matrix form as follows

$$[z\mathbf{I} + \tilde{\mathbf{M}}(k, z = 0)]\tilde{\mathbf{F}}(k, z) = \mathbf{F}(k, t = 0), \tag{4.3}$$

where the 3×3 matrices of time correlation functions $\mathbf{F}(k, t)$, its Laplace transform $\tilde{\mathbf{F}}(k, z)$ and others are defined on the set of three dynamic variables

$$\mathbf{A}^{(hyd)}(k, t) = \left\{n(k, t), J^L(k, t), e(k, t)\right\}, \tag{4.4}$$

where $J^L(k, t)$ and $e(k, t)$ correspond to spatial Fourier components of longitudinal component of density of total momentum and energy density, respectively. The structure of the matrix equation (4.3) exactly corresponds to the Laplace-transformed form of the generalized Langevin equation [7, 14] with the $\tilde{\mathbf{M}}(k, z)$ being the matrix of Laplace-transformed memory functions [16].

Among the eigenmodes of the hydrodynamic model (4.3), (4.4) there are: a single pure real eigenvalue

$$d_1(k) = D_T k^2, \quad Re[z_1](k) = d_1(k),$$

where D_T is thermal diffusivity, and a pair of complex-conjugated eigenvalues

$$z_{\pm}(k) = \Gamma k^2 \pm i c_s k,$$

where the imaginary part corresponds to the hydrodynamic dispersion law

$$\omega(k) = c_s k$$

and real part describes damping of collective excitations with the damping coefficient

$$\Gamma = \frac{1}{2}[D_L + (\gamma - 1)D_T],$$

which depends on thermal diffusivity D_T and longitudinal kinematic viscosity D_L. The eigenvectors associated with the eigenvalues result in amplitudes of mode contributions to the density-density time correlation functions

$$F_{nn}(k, t) = A_{nn} e^{-D_T k^2 t} + [B_{nn} \cos c_s k t + D_{nn}(k) \sin c_s k t] e^{-\Gamma k^2 t}, \tag{4.5}$$

where $A_{nn}(k \to 0) = 1 - \gamma^{-1}$, $B_{nn}(k \to 0) = \gamma^{-1}$ and $D_{nn}(k) = \frac{3\Gamma - D_L}{\gamma c_s} k$.

An important insight for the propagation of macroscopic sound in fluids can be obtained from application of a perturbation approach [17, 18] for cross-correlations in the hydrodynamic model. In particular, if the cross-correlations between thermal and viscous processes are small, i.e. for small ratio of specific heats γ, it is easily to show that the macroscopic sound propagation in fluids is caused by coupled fluctuations of $n(k, t)$ and $J^L(k, t)$ while the cross-correlation with thermal processes renormalizes its propagation speed from the isothermal c_T to the adiabatic c_s value.

4.2.2 Extended Hydrodynamic Approach

In order to account for the short-time dynamic processes on molecular spatial and temporal scales in addition to hydrodynamic ones (which correspond to very small wave numbers and are quite slow) one has to apply generalized hydrodynamics for analysis of time-dependent correlations. A straightforward way is to introduce in addition to the hydrodynamic set of three variables some new ones (non-hydrodynamic variables of fluctuations of non-conserved quantities) which would describe more short-time processes. Suppose that the non-hydrodynamic variables are chosen to be "orthogonal" to the hydrodynamic ones in the sense of statistically independent correlation of corresponding fluctuations, i.e. their cross-correlators are zero

$$< A^{hyd}(-k) A^{non-hyd}(k) > \equiv 0,$$

that allows them to describe dynamic processes in liquids beyond the hydrodynamic regime [7, 14]. Henceforth we will denote by angle brackets an average over the equilibrium canonic ensemble. The most obvious choice for the non-hydrodynamic variables is to sample the first time derivatives of the hydrodynamic ones, because [7]

$$< A(-k) \frac{\partial}{\partial t} A(k) > = < A(-k) \dot{A}(k) > \equiv 0.$$

In [19, 20] it was proposed to generate an extended set of N_v dynamic variables by taking the first and next time derivatives of the hydrodynamic variables, generate the $N_v \times N_v$ generalized hydrodynamic matrix, find its N_v eigenvalues and associated eigenvectors and construct from them the theoretical density-density time correlation function, which can be compared either with the simulation-derived $F_{nn}(k,t)$, or via the time-Fourier transform compared with the experimental dynamic structure factor $S(k,\omega)$. Such an approach is known in the literature as the approach of generalized collective modes (GCM). While the approach of deSchepper and Cohen [19] makes use of fitting parameters connected with unknown wavenumber-dependent transport coefficients, the methodology proposed by Mryglod, Omelyan and Tokarchuk [20] allows to have the unknown for the theory wavenumber dependences of different correlation times $\tau_{ij}(k)$ via their direct estimation in molecular dynamics (MD) simulations. Extensive studies of generalized collective modes [21, 22] showed a convergence of the GCM eigenvalues with systematic extension of the set of dynamic variables up to the third time derivatives of the hydrodynamic ones. The GCM methodology is very close to the generalized hydrodynamic theory by Kivelson and Keyes [23, 24] developed for molecular fluids. The microscopic theory of extended collective modes enables correct description of the hydrodynamic modes as well as of the well-defined short-wavelength collective excitations for large wave numbers [25, 26].

In general within the GCM approach the extended set of N_v dynamic variables is used for estimation of the matrix elements of the generalized hydrodynamic matrix $\mathbf{T}(k)$ obtained from the matrix of time correlation functions $\mathbf{F}(k,t)$ and its Laplace transform $\tilde{\mathbf{F}}(k,z)$ taken in Markovian approximation $(z=0)$

$$\mathbf{T}(k) = \mathbf{F}(k,t=0)\tilde{\mathbf{F}}^{-1}(k,z=0). \tag{4.6}$$

The N_v eigenvalues and associated eigenvectors yield GCM expression for any time correlation function between two dynamic variables of the given set of N_v ones via a separable sum of contributions from N_v collective modes

$$F_{ij}^{GCM}(k,t) = \sum_{\alpha}^{N_v} G_{ij}^{\alpha}(k) e^{-z_\alpha(k)t}. \tag{4.7}$$

Here the sum is over N_v mode contributions, the $z_\alpha(k)$ and weight coefficients $G_{nn}^{\alpha}(k)$ are in general case complex functions of wave number k. The mode contributions can be transformed to purely real weight coefficients as it was proposed in [27].

Very important is the issue of exact sum rules which should satisfy the theoretical time correlation functions $F_{ij}(k,t)$. Any time correlation function between dynamic variables of the classical system has the following short-time expansion [7, 14]

$$F_{ij}(k,t) = F_{ij}(k,t=0)[1 - \frac{1}{2!}\langle\omega^2\rangle_{ij}(k)t^2 + \frac{1}{4!}\langle\omega^4\rangle_{ij}(k)t^4 - \frac{1}{6!}\langle\omega^6\rangle_{ij}(k)t^6 + \ldots]. \tag{4.8}$$

Here the wavenumber-dependent coefficients $\langle\omega^{2n}\rangle_{ij}(k)$, $n = 0, 1, 2, \ldots$ are the normalized $2n$th frequency moments of corresponding spectral function (dynamic structure factor for the case of density-density fluctuations)

$$\langle\omega^{2n}\rangle_{ij}(k) = \frac{1}{2\pi F_{ij}(k,t=0)} \int_{-\infty}^{\infty} \omega^{2n} S_{ij}(k,\omega) d\omega. \tag{4.9}$$

Since the dynamic structure factors are even functions of frequency for classical systems—all odd frequency moments are equal to zero

$$\langle\omega^{2n+1}\rangle_{ij}(k) \equiv 0 \quad n = 0, 1, 2, \ldots$$

For the density-density time correlation functions there exist exact analytical expressions for first eight frequency moments [7]. The zeroth and second frequency moments in the expansion of the density-density time correlation function have very simple form

$$\langle \omega^0 \rangle_{nn}(k) \equiv 1, \quad \langle \omega^2 \rangle_{nn}(k) = \frac{k_B T}{m S(k)} k^2.$$

The higher even frequency moments of dynamic structure factor are expressed via spatial integrals involving effective interactions and their spatial derivatives [7, 14]. The extended sets of dynamic variables enable derivation of theoretical expressions for time correlation functions (4.7) with different level of the sum rules fulfilled. As it was shown in [20] if the model included in the extended set of variables all time derivatives of a hydrodynamic variable $A(k,t)$ up to the sth order, then the corresponding GCM time correlation function $F_{AA}^{GCM}(k,t)$ would exactly fulfill first $2s+1$ sum rules for corresponding frequency moments.

The eigenvalues and corresponding eigenvectors of the generalized hydrodynamic matrix represent the dynamic eigenmodes that can exist in fluids on the spatial scale $\sim 2\pi/k$ for the given wave number k. The eigenvalues of $\mathbf{T}(k)$ are either real numbers $d_\alpha(k)$ or pairs of complex-conjugated numbers $z_\alpha(k) = \sigma_\alpha(k) \pm i\omega_\alpha(k)$. The formers correspond to relaxing mode with the relaxation time $d_\alpha^{-1}(k)$, while the latters—to propagating modes with dispersion $\omega_\alpha(k)$ and damping $\sigma_\alpha(k)$. The GCM methodology was developed in spirit of the traditional for solids eigenvalue problem for dynamic matrix, however it is free from an assumption of local potential energy minima for atoms and additionally allows to study relaxing modes and their effects on the dispersion of collective excitations. Analysis of the dispersion $\omega(k)$ of acoustic modes should clarify the issue of the existence and behaviour of positive sound dispersion and non-hydrodynamic modes in supercritical fluids in very wide range of densities.

In the long-wavelength limit one knows the exact asymptotes of the correlation times and different correlators, that allows analytical studies of non-hydrodynamic collective modes in fluids [28]. Below we will show how analytical results can be obtained within the GCM approach for the positive sound dispersion in supercritical fluids. The GCM approach was successfully applied in analytical theories of non-hydrodynamic optic-like excitations in binary liquids [29, 30], "fast sound" excitations in binary liquids with disparate masses [31] and propagating charge modes in molten salts [32], and all the analytical results were supported by the MD simulations.

4.2.3 Viscoelastic Model

A simple dynamical model for longitudinal dynamics of fluids, which consists of three dynamical variables

$$\mathbf{A}^{(ve)}(k,t) = \left\{ n(k,t), J^L(k,t), \dot{J}^L(k,t) \right\}, \tag{4.10}$$

is well known as the viscoelastic one, because in addition to the hydrodynamic variables of particle density and longitudinal component of mass-current density, a non-hydrodynamic variable connected with the elastic properties of the liquid is taken into account. Since the extended variable $\dot{\mathbf{J}}(k,t)$ is connected to the stress tensor $\sigma_{\alpha\beta}(k,t)$ via [33]:

$$\frac{d}{dt}\mathbf{J}(k,t) = i\mathbf{k}\hat{\sigma}(k,t),$$

there appear in the viscoelastic approach the elastic quantities connected with microscopic forces acting on particles. From the point of view of exact sum rules the density-density time correlation function obtained from this model will have exact first five sum rules satisfied, that is two more than within the hydrodynamic description.

In this set of dynamic variables $\mathbf{A}^{(ve)}(k,t)$ one does not take the energy fluctuations into account, hence the density-density correlation time can be obtained from the hydrodynamic one $\tau_{nn}(k)$ defined as

$$\tau_{nn}(k) = \frac{1}{S(k)}\int_0^\infty F_{nn}(k,t)dt$$

by setting $\gamma = 1$ in the analytical hydrodynamic expression for $F_{nn}(k,t)$ [9]:

$$\tau_{nn}(k) = \frac{D_L}{c_s^2 + 4D_L^2k^2}.$$

Now the generalized hydrodynamic matrix generated on the basis set (4.10) can be written down as follows:

$$\mathbf{T}^{(ve)}(k) = \begin{pmatrix} 0 & -i\frac{k}{m} & 0 \\ 0 & 0 & -1 \\ -imkc_T^2\frac{c_\infty^2 - c_T^2}{D_L} & k^2c_\infty^2 & \frac{c_\infty^2 - c_T^2}{D_L} \end{pmatrix}, \tag{4.11}$$

where the following shortcut was introduced $k^2c_\infty^2 = \langle \dot{J}^L\dot{J}^L\rangle / \langle J^L J^L\rangle$ with c_∞ being the high-frequency (elastic) speed of sound. The quantities D_L and c_T in (4.11) are the kinematic viscosity and isothermal speed of sound. One can easily find eigenvalues of the matrix $\mathbf{T}^{(ve)}(k)$ within the precision of $O(k^2)$, which are a pair propagating modes

$$z_\pm(k) = \frac{D_L}{2}k^2 \pm ic_Tk \equiv \sigma(k) \pm i\omega(k), \tag{4.12}$$

and a non-hydrodynamic relaxing collective mode

$$d_{ve}(k) = \frac{c_\infty^2 - c_T^2}{D_L} - D_L k^2 \equiv d^0 - D_L k^2, \tag{4.13}$$

which tends to a nonzero constant d^0 in the long-wavelength limit. The factor $(c_\infty^2 - c_T^2)$ is usually called as the "strength" of the structural relaxation process. Besides, the constant d^0 goes to zero when the kinematic viscosity tends to infinity, that means an almost infinite relaxation time of the mode $d_{ve}(k)$ at the glass transition. All this implies, that the non-hydrodynamic mode $d_{ve}(k)$ is connected to the structural relaxation.

The expression for the sound dispersion (imaginary part of eigenvalues $z_\pm(k)$) does not show any effect due to coupling of acoustic excitations with the non-hydrodynamic mode of structural relaxation $d_{ve}(k)$, that can appear only in the $O(k^3)$ order in the sound dispersion. In order to estimate the imaginary part of the complex eigenvalues corresponding sound dispersion within the precision of $O(k^3)$ one can derive from (4.11) an effective equation for sound eigenmodes by eliminating the known real eigenvalue $d_{ve}(k)$ (4.13). The effective equation reads

$$z^2 - D_L k^2 z + \frac{c_T^2 d^0}{d_{ve}(k)} k^2 = 0, \tag{4.14}$$

and now the sound dispersion can be obtained as

$$\omega_{ve}(k) = c_T k \sqrt{1 + \frac{D_L}{d^0} k^2 - \frac{D_L^2}{4c_T^2} k^2 + O(k^4)} = c_T k + \beta_{ve} k^3 + \ldots \tag{4.15}$$

In the expression under the square root there are two contributions proportional to k^2: the first one is positive and comes from the coupling of acoustic excitations with structural relaxation, and the second contribution, the negative one, is the standard renormalization down of the dispersion law due to the damping effects. One can obtain the first correction to the linear viscoelastic dispersion law, proportional to the k^3 having the following coefficient:

$$\beta_{ve} \approx c_T \frac{D_L^2}{8} \frac{5 - (c_\infty / c_T)^2}{c_\infty^2 - c_T^2}. \tag{4.16}$$

The most interesting consequence is, that in general the sign of the $O(k^3)$ correction to the linear dispersion law can be different depending on the ratio between the high-frequency speed of sound and the isothermal one. Note, that the high-frequency speed of sound is always higher than the adiabatic one c_s [34, 35], which in its turn is $\sqrt{\gamma}$ times higher than c_T.

For the case of transverse dynamics the viscoelastic model contains just two dynamic variables

$$\mathbf{A}^{(ve,T)}(k,t) = \left\{J^T(k,t), \dot{J}^T(k,t)\right\}. \tag{4.17}$$

These two dynamic variables can be used for estimation of the 2×2 generalized hydrodynamic matrix for the transverse case. The two eigenmodes for this model easily can be obtained [28, 36] in the whole range of wave numbers. In the long-wavelength region they are purely real eigenvalues corresponding to two (one hydrodynamic and one non-hydrodynamic) relaxing modes, while starting from a nonzero wave number

$$k_s = \frac{\sqrt{\rho G}}{2\eta}, \tag{4.18}$$

where G and η are the high-frequency shear modulus and shear viscosity, respectively, in the fluid emerge short-wavelength shear waves (a pair of complex-conjugated eigenvalues of the generalized hydrodynamic matrix for the transverse dynamics). The long-wavelength region $k < k_s$ in which the transverse collective excitations are not supported by the fluid is called a propagation gap for shear waves. The dispersion of the shear waves is

$$\omega^T(k) = \left[\langle\omega^2\rangle_{JJ}(k) - \sigma^2(k)\right]^{1/2}, \tag{4.19}$$

where the second frequency moment of the transverse current-current spectral function

$$\langle\omega^2\rangle_{JJ}(k) = k^2 G(k)/\rho \equiv \frac{\langle\dot{J}^T(-k)\dot{J}^T(k)\rangle}{\langle J^T(-k)J^T(k)\rangle}$$

should be larger than the square of the damping coefficient $\sigma(k)$ in order the shear waves to exist. The $G(k)$ in the expression above is the wavenumber-dependent shear modulus which tends to its macroscopic value G in the long-wavelength limit. It is seen that for small wave numbers the second frequency moment of the transverse current-current spectral function tends to zero resulting in the negative expression under the square root in (4.19) that corresponds to the region where no transverse propagating modes can exist in the fluid.

4.2.4 Thermoviscoelastic Approach

Now we will take into account the coupling of density fluctuations to thermal processes and find out how this effect contributes to the deviation of the dispersion curve from the linear hydrodynamic dispersion law. We want to obtain the analytical expressions for the eigenmodes in a pure fluid, within a five-variable thermo-viscoelastic model in the long-wavelength limit [37]. The dynamical model $\mathbf{A}^{(5)}(k,t)$

$$\mathbf{A}^{(5)}(k,t) = \left\{n(k,t), J^L(k,t), e(k,t), \dot{J}^L(k,t), \dot{e}(k,t)\right\} \tag{4.20}$$

contains additionally to the viscoelastic model the energy density $e(k,t)$ and the corresponding extended variable $\dot{e}(k,t)$. The five eigenmodes within the precision of $O(k^2)$ for the thermo-viscoelastic model were reported in [37] and contained three hydrodynamic modes:

$$\begin{aligned} d_1(k) &= D_T k^2, \\ z_{\pm}(k) &= \Gamma k^2 \pm i[c_s k + O(k^3)], \end{aligned} \tag{4.21}$$

exactly as they appear in the hydrodynamic approach, and two non-hydrodynamic relaxing modes:

$$d_2(k) = d_2^0 - D_L k^2 + (\gamma - 1)\Delta k^2, \tag{4.22}$$

and

$$d_3(k) = d_3^0 - \gamma D_T k^2 - (\gamma - 1)\Delta k^2, \tag{4.23}$$

where the following shortcuts were introduced:

$$d_2^0 = \frac{c_\infty^2 - c_s^2}{D_L},$$

and

$$d_3^0 = \frac{C_V}{m\lambda}[G^h - \frac{(\gamma - 1)}{\kappa_T}],$$

and

$$\Delta = \frac{d_2^0 d_3^0}{d_3^0 - d_2^0}\frac{D_T}{D_L c_s^2}(D_T - D_L)^2.$$

The G^h corresponds to the heat rigidity modulus and λ is the thermal conductivity. The last terms in right hand sides of (4.22) and (4.23) appear only due to coupling between the heat and density fluctuations. When this coupling is neglected, i.e. $\gamma = 1$, one obtains for the non-hydrodynamic modes $d_2(k)$ and $d_3(k)$ the same expressions as within the separated treatment of two-variable heat—and three-variable viscoelastic dynamical models (at $\gamma = 1$ the non-hydrodynamic mode $d_2(k)$ is reduced to (4.13)).

The complex eigenvalues of the thermo-viscoelastic dynamic model within the precision of $O(k^3)$ are

$$z_s(k) = \Gamma k^2 \pm i(c_s k + \beta k^3), \tag{4.24}$$

where the coefficient at k^3 reads as follows:

$$\beta = -\frac{\Gamma^2}{2c_s} - (\gamma - 1)D_T \frac{D_L - D_T}{2c_s} + \frac{c_s D_L}{2d_2^0} + (\gamma - 1)\frac{c_s(\gamma - 1)D_T}{2d_3^0}. \tag{4.25}$$

In the case when $\gamma \approx 1$ the estimate for the sound dispersion at the boundary of hydrodynamic regime within the thermo-viscoelastic model reads:

$$\omega(k) \approx c_s k + \frac{c_s D_L^2}{8} \frac{5 - (c_\infty / c_s)^2}{c_\infty^2 - c_s^2} k^3, \tag{4.26}$$

which is identical to (4.15) and (4.16) for the case of $\gamma = 1$, with c_s being equal to c_T.

4.3 Computer Simulations of Time-Dependent Correlations

Computer molecular dynamics simulations represent a powerfull tool which being based on laws of microscopic statistical mechanics is in fact a computer experiment for realistic systems, that allows direct comparison with the output of real experiments. The time correlation functions directly obtained in MD simulations can be compared via the time-Fourier transform with the experimentally measured dynamic structure factor $S(k, \omega)$. The dispersion of collective excitations can be obained either directly from observation of the locations of the visible Brillouin peaks (4.1) in dynamic structure factor, or from a fitting procedure based either on a simple model of damped harmonic oscillator (DHO) [38, 39] or expressions for dynamic structure factor obtained within second order memory function approach [7, 14]. The direct observation of the Brillouin peaks is not really precise methodology because they are well-pronounced only for essentially small wave numbers. Therefore the main approach of the direct estimation from MD of the dispersion of collective excitations is from the peak position in the longitudinal current spectral function $C^L(k, \omega)$, which according to the continuity equation has the following relation with the dynamic structure factor [7, 14]

$$C^L(k, \omega) = \frac{\omega^2}{k^2} S(k, \omega). \tag{4.27}$$

The methodology based on identification of the dispersion of collective excitations with the peak locations of $C^L(k, \omega)$ also has its drawbacks connected with the neglect of contributions from relaxation processes to $C^L(k, \omega)$. The strong contributions from relaxation processes can essentially shift the contribution from

collective excitations and therefore the apparent peak position of $C^L(k,\omega)$ can essentially differ from the real frequency of the collective excitation.

Therefore more advanced methods of estimation of dispersion of collective excitations in fluids are based on theoretical expressions for the time correlation functions or $S(k,\omega)$ and $C^L(k,\omega)$ obtained within generalized hydrodynamic approach. The theoretical expressions are either fitted (memory function approach) or directly compared without any fit (GCM approach) with the simulation data. Several fitting schemes were proposed for the density-density time correlation functions or dynamic structure factors within different approximations for memory functions [40–47] with the purpose to estimate dispersion of collective excitations in liquids while parameter-free calculation of the dispersion was developed only within the GCM approach.

In order to perform analysis of collective dynamics from MD simulations one has to calculate hydrodynamic time correlation functions. For this purpose one has to sample in MD simulations the spatial Fourier components of density of hydrodynamic quantities: number density of particles

$$n(k,t) = \frac{1}{\sqrt{N}} \sum_{j=1}^{N} e^{i\mathbf{k}\mathbf{r}_j(t)}, \tag{4.28}$$

where $\mathbf{k}$ is the sampled wave vector and $\mathbf{r}_j(t)$ is the trajectory of the jth particle; longitudinal and transverse components of momentum density

$$\begin{aligned} J^L(k,t) &= \frac{m}{k\sqrt{N}} \sum_{i=1}^{N} \mathbf{k}\mathbf{v}_j(t) e^{i\mathbf{k}\mathbf{r}_j(t)}, \\ \mathbf{J}^T(k,t) &= \frac{m}{k\sqrt{2}\sqrt{N}} \sum_{j=1}^{N} [\mathbf{k} \times \mathbf{v}_j(t)] e^{i\mathbf{k}\mathbf{r}_j(t)}, \end{aligned} \tag{4.29}$$

and energy density

$$e(k,t) = \frac{1}{\sqrt{N}} \sum_{j=1}^{N} \varepsilon_j(t) e^{i\mathbf{k}\mathbf{r}_j(t)}. \tag{4.30}$$

In (4.29) and (4.30) $\mathbf{v}_j$ and ε_j are the velocity and single-particle energy of the jth particle. Note that the dynamic variables of number density and longitudinal component of momentum density are connected by the fundamental continuity equation

$$\frac{dn(k,t)}{dt} = \frac{ik}{m} J^L(k,t). \tag{4.31}$$

The extended dynamic variables are obtained from (4.29) and (4.30) as their first time derivatives:

$$\dot{J}^L(k,t) = \frac{m}{k\sqrt{N}} \sum_{j=1}^{N} [\mathbf{k}\mathbf{a}_j(t) + i[\mathbf{k}\mathbf{v}_j(t)]^2] e^{i\mathbf{k}\mathbf{r}_i(t)},$$

$$\dot{\mathbf{J}}^T(k,t) = \frac{m}{k\sqrt{2}\sqrt{N}} \sum_{j=1}^{N} [\mathbf{k} \times \mathbf{a}_j(t) + i[\mathbf{k} \times \mathbf{v}_j(t)]\mathbf{k}\mathbf{v}_j(t)] e^{i\mathbf{k}\mathbf{r}_j(t)},$$

$$\dot{e}(k,t) = \frac{1}{\sqrt{N}} \sum_{j=1}^{N} [\dot{\varepsilon}_j(t) + i\varepsilon_j(t)\mathbf{k}\mathbf{v}_j(t)] e^{i\mathbf{k}\mathbf{r}_j(t)},$$

where the overdot means the time derivative and $\mathbf{a}_j(t)$ is the acceleration of the jth particle.

The density-density time correlation functions $F_{nn}(k,t)$ in different regions of wave numbers are shown for supercritical Ar at $T = 280\,\mathrm{K}$ and density $921.885\,\mathrm{kg/m^3}$ in Fig. 4.1. The MD simulations [48] were performed for 13 densities along the isothermal line $T = 280\,\mathrm{K}$ for supercritical Ar using systems of 2000 particles interacting via ab initio Woon potentials [49]. Parameters of the potentials were taken from [50] and cut-off radius was 12 Å. These potentials were the same as used in the experimental and MD study of supercritical Ar at 573 K [5]. The time step in simulations was 2 fs. All the simulations were performed in microcanonical ensemble. Energy conservation was on very good level: the energy drift was less than 0.02 percent over the production runs of 480,000 time steps. Every sixth configuration was used for sampling of dynamic variables. Dynamic variables of particle density, momentum density and energy density as well as their time derivatives needed for GCM analysis were sampled for thirty different wave numbers directly in MD simulations. The averages of static and time correlation functions over all possible directions of different wave vectors with the same magnitude were performed.

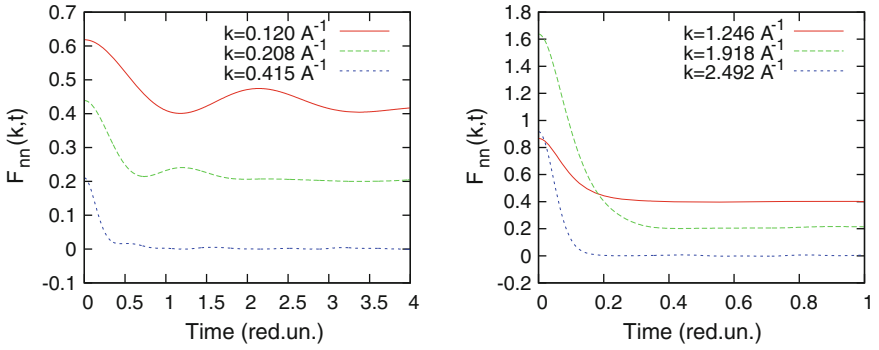

Fig. 4.1 Density-density time correlation functions for supercritical Ar at $T = 280\,\mathrm{K}$ and density $921.885\,\mathrm{kg/m^3}$ at six wave numbers as directly obtained in MD simulations. The time scale for reduction of units is 3.45494276 ps. A progressive vertical shift of 0.2 was applied with decreasing wave numbers for eye convenience

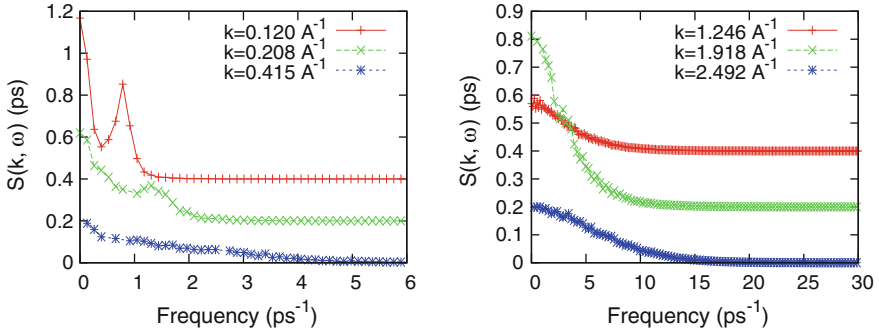

Fig. 4.2 Dynamic structure factors for supercritical Ar at 280 K at six wave numbers obtained from time-Fourier transformation of corresponding density-density time correlation functions shown in Fig. 4.1. A progressive vertical shift of 0.2 was applied with decreasing wave numbers for eye convenience

In Fig. 4.1 one can see that only for very small wave numbers the density-density time correlation functions show oscillating behaviour due to propagating collective excitations, while with increasing wave numbers the oscillations got hidden under the relaxation shape of the $F_{nn}(k,t)$. It is obvious that the purely relaxation shape of $F_{nn}(k,t)$ as is observed for $k > 0.5$ Å^{-1} for this thermodynamic point of supercritical Ar does not mean the absence of collective excitations. The corresponding dynamic structure factors are shown in Fig. 4.2. According to the Landau-Placzek ratio the visibility of the side Brillouin peaks depends on the ratio of specific heats γ, which was obtained in [48] from MD simulations for this thermodynamic point $\gamma = 1.98$ in good agreement with the NIST database [51]. It is seen from Fig. 4.2 that is is impossible to observe the exact location of the side peak of $S(k,\omega)$ for wave numbers $k > 0.3$ Å^{-1} that excludes the possibility to estimate dispersion of collective excitations for these wave numbers directly from the obtained dynamic structure factors.

Since the fluctuations of density are connected with the fluctuations of the longitudinal mass-current density via the time derivative of the former, the time correlation functions $F^L_{JJ}(k,t)$ show well pronounced oscillations (Fig. 4.3) in the region of small wave numbers. However even far outside the hydrodynamic region the longitudinal current-current time correlation functions show negative minimum at small times that is an evidence of the presence of collective excitations in contrast to what was observed in the shape of the density-density time correlation functions at large wave numbers.

The time-Fourier transform of $F^L_{JJ}(k,t)$, which is denoted as $C^L(k,\omega)$, shows the well-pronounced maximum as a function of frequency for all wavenumbers as it is seen from Fig. 4.4. The maxima positions of $C^L(k,\omega)$ give the direct, though being exact only in the long-wavelength limit and therefore—not really precise for large wave numbers, way of estimation of the dispersion $\omega(k)$ of longitudinal collective excitations in fluids.

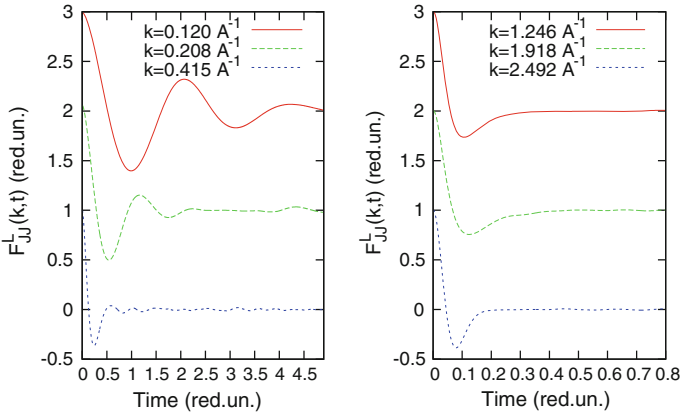

Fig. 4.3 Longitudinal current-current time correlation functions for supercritical Ar at $T = 280\,\mathrm{K}$ and density $921.885\,\mathrm{kg/m^3}$ at six wave numbers as directly obtained in MD simulations. The time scale for reduction of units is 3.45494276 ps. A progressive vertical shift of 1.0 was applied with decreasing wave numbers for eye convenience

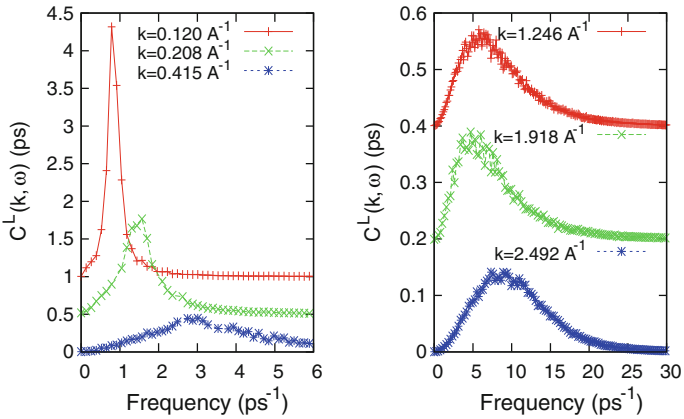

Fig. 4.4 Longitudinal current spectral functions $C^L(k,\omega)$ for supercritical Ar at $T = 280$ K and density $921.885\,\mathrm{kg/m^3}$ at six wave numbers as directly obtained in MD simulations. A progressive vertical shifts of 0.5 and 0.2 were applied in the left and right frames with decreasing wave numbers for eye convenience

The ability of the generalized hydrodynamics to describe correctly the time-dependent correlations are shown in Fig. 4.5, where density-density, density-energy and energy-energy time correlation functions obtained from MD simulations are compared without any fit with the corresponding functions obtained within the five-variable thermo-viscoelastic GCM approach (4.20). The theoretical curves (4.7) almost perfectly recover the damped oscillations in the shape of the MD-derived time correlation functions and nicely reproduce their short-time

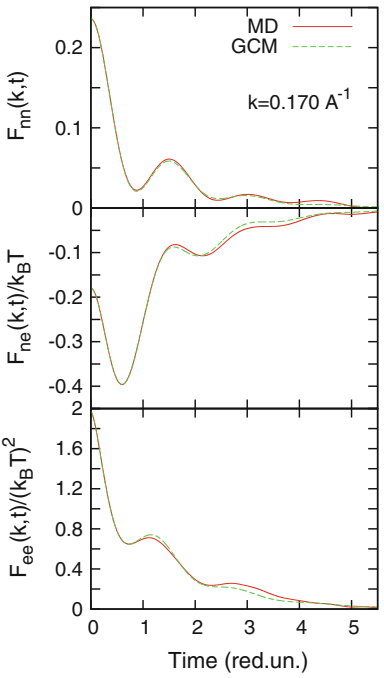

Fig. 4.5 Density-density, density-energy and energy-energy time correlation functions obtained from MD simulations (*solid line*) and from fit-free thermo-viscoelastic (20) generalized hydrodynamic GCM approach (*dashed line*) for supercritical Ar at $T = 280\,\mathrm{K}$ and density $1621.2\,\mathrm{kg/m^3}$

behaviour due to high number of the sum rules fulfilled. This means that the five-variable thermo-viscoelastic model is able to yield correct dispersion of the collective excitations in fluids.

Transverse dynamics can be studied via analysis of the transverse current-current time correlation functions $F_{JJ}^{T}(k,t)$, shown for six wave numbers in Fig. 4.6. An analytical expression for the $F_{JJ}^{T}(k,t)$ that follows from hydrodynamic theory [7] is valid only for small wave numbers:

$$F_{JJ}^{T,hyd}(k,t) = \frac{k_B T}{m} e^{-\frac{\eta k^2}{\rho} t}, \tag{4.32}$$

where η is shear viscosity. In Fig. 4.6 the time correlation function $F_{JJ}^{T}(k,t)$ with the smallest wave number corresponds well to the single-exponential hydrodynamic form (4.32). However outside the hydrodynamic region a deviation from the hydrodynamic form is increasing. For very dense fluids outside the hydrodynamic region a similar as in longitudinal case (Fig. 4.3) negative minimum at small times is observed, which is an evidence of emerging in the liquid short-wavelength shear waves [29, 36].

The time-Fourier transformed transverse functions $F_{JJ}^{T}(k,t)$ give transverse current spectral functions $C^{T}(k,\omega)$ shown in Fig. 4.7. In contrast to the longitudinal case $C^{T}(k,0) \neq 0$, hence for the transverse spectral functions $C^{T}(k,\omega)$ the contributions from transverse collective excitations can be hidden under the relaxing

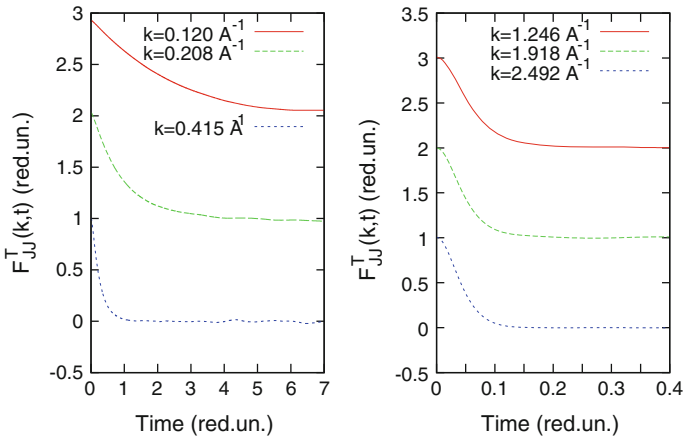

Fig. 4.6 Transverse current-current time correlation functions for supercritical Ar at $T = 280\,\mathrm{K}$ and density $921.885\,\mathrm{kg/m^3}$ at six wave numbers as directly obtained in MD simulations. The time scale for reduction of units is 3.45494276 ps. A progressive vertical shift of 1.0 was applied with decreasing wave numbers for eye convenience

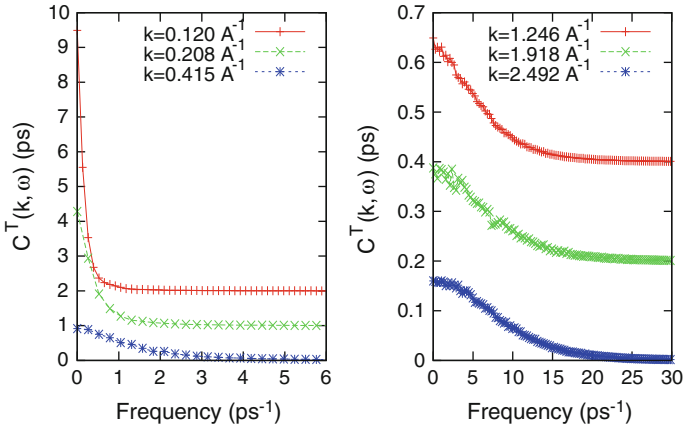

Fig. 4.7 Transverse current spectral functions $C^T(k,\omega)$ for supercritical Ar at $T = 280\,\mathrm{K}$ and density $921.885\,\mathrm{kg/m^3}$ at six wave numbers as directly obtained in MD simulations. A progressive vertical shifts of 1.0 and 0.2 were applied in the left and right frames with decreasing wave numbers for eye convenience

part of $C^T(k,\omega)$. Indeed, the zero-frequency limit of the transverse spectral functions reads $C^T(k,0) \sim \rho/(k^2\eta(k))$, where $\eta(k)$ is the wavenumber-dependent shear viscosity, which tends in the long-wavelength limit to its macroscopic value η. The issue of the visibility of transverse collective excitations in $C^T(k,\omega)$ is not really well elaborated in the literature, but it is obvious that the absence of the well-defined peak in $C^T(k,\omega)$ does not mean the complete absence of shear waves

propagating on nanoscales $L \sim 2\pi/k$. Similarly, the absence of a side peak in dynamic structure factors $S(k,\omega)$ for large wave numbers does not mean the absence of short-wavelength longitudinal collective excitations. In fact their contribution simply is too weak in comparison with the one from relaxation processes. Therefore in the case of transverse dynamics only the proper analysis based on dynamic eigenmode calculations can reveal the existence of transverse excitations, their dispersion and contribution to $C^T(k,\omega)$ in a wide range of densities.

The two-variable viscoelastic model of transverse dynamics (4.17) is able to fulfill only first three frequency moments of the transverse current spectral function, therefore the theoretical curves recover the MD-derived transverse time correlation functions not so perfectly as it is for the longitudinal case. One should note that the short-time behaviour of the transverse time correlation functions is exactly the same as for the regular time correlation function (4.8) and depends on the first few k-dependent frequency moments. The long-time behaviour though is different in the small-k and large-k limits. While in the hydrodynamic regime the transverse current functions have typical single-exponential decay, in the limit of large wave numbers these function should have Gaussian-type tail of the time dependence [7]. In Fig. 4.8 theoretical and MD-derived transverse time correlation functions are compared for three wave numbers. One can see that close to the hydrodynamic region the quality of theory is very good, while in the region where exist shear waves the theoretical curves correctly recover the frequency of damped oscillation, but underestimate their damping. In general one can expect that further extension of the two-variable set of transverse dynamics would allow better description of the damping of shear waves. Note that for the highest wave number shown in Fig. 4.8 the Gaussian regime for the long-time behaviour has not been reached.

Having the eigenvalues obtained from the generalized hydrodynamic matrix in the longitudinal and transverse cases one can compare the dispersion of the eigenmodes with the dispersion curves estimated from the peak positions of current spectral functions $C^{L/T}(k,\omega)$. In Fig. 4.9 one observes deviation of the dispersion of longitudinal collective excitations from the linear hydrodynamic dispersion law

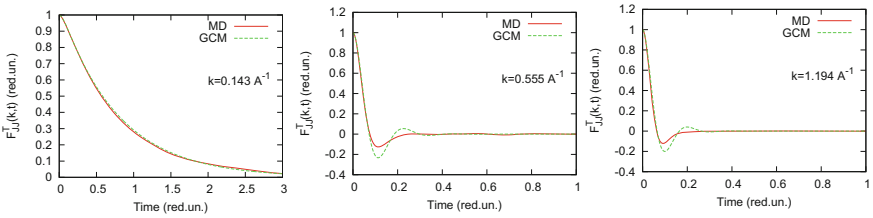

Fig. 4.8 Transverse current-current time correlation functions for three wave numbers as obtained from MD simulations (*solid line*) and from the fit-free viscoelastic (4.17) generalized hydrodynamic GCM approach (*dashed line*) for supercritical Ar at $T = 280\,\mathrm{K}$ and density $1621.2\,\mathrm{kg/m^3}$

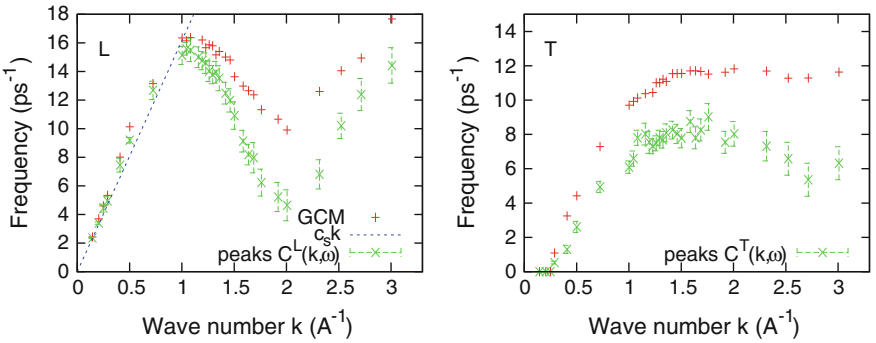

Fig. 4.9 Dispersion of longitudinal (L) and transverse (T) collective excitations for supercritical Ar at $T = 280$ K and density 1621.2 kg/m^{3}obtained from the peak positions of the L-and T-current spectral functions (cross symbols with error bars) and from the theoretical thermo-viscoelastic (4.20) and viscoelastic (for T) models of collective dynamics (plus symbols)

in perfect agreement of theory and MD simulations, that is an evidence of correct description of the positive sound dispersion within the thermo-viscoelastic dynamic model. The macroscopic adiabatic speed of sound c_s is not an easy task to estimate from molecular dynamics simulations. We used one of the most reliable approaches to calculate c_s via the long-wavelength extrapolation of a smooth dependence $\sqrt{\gamma(k)/S(k)}$ multiplied by the thermal velocity. Here $\gamma(k)$ is the wavenumber-dependent ratio of specific heats which easily can be expressed via correlators used in the GCM approach [20, 52]. To date this is the most precise methodology of calculations of adiabatic speed of sound from classical [35, 48] and ab initio [53–55] simulations. A comparison of the calculated adiabatic speed of sound for supercritical Ar with the NIST database showed almost perfect agreement in the whole density range, see [48].

For the transverse case both the GCM theory and MD simulations are in nice agreement for the existence and the width of the propagation gap for shear waves. In the region of wave numbers where the density-density time correlation functions show relaxing behaviour with no oscillations the peak positions of $C^L(k,\omega)$ are located at smaller frequencies with respect to the dispersion obtained from GCM eigenmodes, that is explained by the neglect of the shift of the frequency to the apparent one by contributions from relaxing modes. Similar tendency is observed also for the transverse case. This means that the dispersion of collective excitations should be estimated with the full account for different contributions to $C^{L/T}(k,\omega)$ spectral functions from all relaxing and propagating modes, that would allow separation of actual contribution from L/T collective excitations to the $C^{L/T}(k,\omega)$. Namely the GCM approach allows such a separation of different contributions to the spectral functions of interest. In any case the region, where the positive sound dispersion and emergence of shear waves are observed can be studied by different methodologies, because they lead to consistent results for dispersion of collective excitations.

4.4 Crossover in Collective Dynamics of Supercritical Fluids

Attempts to identify liquid-like and gas-like features in supercritical fluids have been undertaken since the derivation of the van der Waals equation of state. More recent approaches targeted on static density fluctuations [56] or suggested a continuous phase transformation in the supercritical region [57, 58]. In particular, in [58] a mesophase in a finite density range separating the low-density gaseous and high-density liquid phases in supercritical region was studied.

Here we will focus on dynamic manifestations of the possible crossover. A crossover in collective dynamics from gas-like to liquid-like behaviour was suggested in [5] on the basis of experimental study of positive dispersion of collective excitations in supercritical Ar. The idea was based on observation that the positive sound dispersion practically vanished at some low density of the supercritical fluid, that led to a suggestion that the dense fluids have liquid-like type of dynamics with nonzero PSD. This was supported by analytical treatment of the positive sound dispersion caused by coupling of acoustic excitations to structural relaxation [34]. Later on another specific non-zero positive dispersion was found in MD simulations of supercritical Argon for low-density states [59]. In was found in [59] that a weak positive deviation from the hydrodynamic dispersion remains even for the low-density supercritical fluids, however it is not anymore connected with the structural relaxation but with coupling with non-hydrodynamic heat waves which can emerge in fluids on short wave lengths. The coupling to heat waves causes the "residual PSD" far outside the hydrodynamic region. If the PSD was solely caused by the structural relaxation it would vanish as it was shown in [34, 35] within the viscoelastic (no coupling with thermal processes) analysis of PSD. In Fig. 4.10 one can observe how the PSD changes with reduction of the density for the case of supercritical Ar. The apparent speed of sound estimated as $\omega_{sound}(k)/k$ shows rapid increase in the long-wavelength region for the high-density fluid, while decreasing density causes much wider region of small wave numbers in which the dispersion remains linear with k. Simulations performed in [34] showed that further

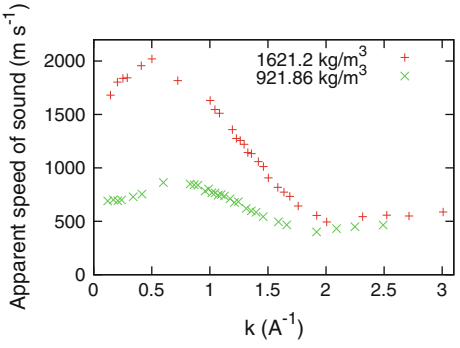

Fig. 4.10 Apparent speed of sound $c_{app}(k) = \omega_{sound}(k)/k$ for two densities of supercritical Ar at $T = 280\,\mathrm{K}$

reduction of the density can cause even a region with "negative" sound dispersion, possibility of which is also supported by expressions (4.15) and (4.26).

Interestingly, that for model fluids of soft spheres, which do not have liquid-gas coexistence, the density dependence of collective dynamics was found very similar as in the supercritical Ar [35]. The apparent speed of sound calculated for soft sphere fluids [35] gives evidence of a strong positive dispersion for the dense fluids and its reduction with the decrease of density reaching almost zero-PSD state at some density. Further decrease of density for soft sphere fluids resulted again in non-zero PSD, that gives evidence of very similar scenario of behaviour of PSD as it was observed in the case of Lennard-Jones fluids [5, 59]. This means that for the systems with and without the gas-liquid binodal and critical point the behaviour of the PSD is very similar.

In order to make a link between the dynamics of systems with and without the coexistence gas-liquid binodal in [35] were calculated density dependences of the thermal diffusivity D_T and of the longitudinal kinematic viscosity D_L. Their density dependences were obtained qualitatively similar with a minimum right at the density where the vanishing PSD was observed. For the soft sphere fluids was obtained similar density dependence of D_T as it was known for real supercritical fluids [51] and were reported in studies of critical behaviour of thermal diffusivity D_T of CO_2, C_2H_6 [60] and H_2O [61]. Both quantities D_T and D_L define the behaviour of the PSD as it follows from the analytical expression reported in 4.25. On the other hand, in more realistic Lennard-Jones supercritical fluids (see [59]) minima in D_T and D_L have been found to correspond to maxima in the specific heat C_P. Note that in the soft sphere fluids the Widom line is no longer defined (no gas-liquid coexistence line and its continuation into supercritical regime) however a link between high frequency dynamics and macroscopic transport/thermodynamic quantities is retained. Put in different words, when soft sphere potential is turned into the Lennard-Jones one by adding the attractive part, the correspondence between the dynamic crossover in PSD and the Widom line is reproduced. In this sense, the soft sphere fluids support such a relationship. For realistic fluids the critical behaviour of the thermal diffusivity

$$D_T = \frac{\lambda}{nC_P}$$

depends on the divergence of thermal conductivity λ and specific heat at constant pressure C_P at the critical point [62]. The experiments [60, 61] give evidence of a rapid decay of D_T on approaching the critical point, i.e. leading contribution from the C_P, and consequently, the line of the minimum of $D_T(n)$ for realistic fluids should be very close to their Widom line. This makes a strong argument in connecting the dynamic crossover in system with and without coexistence gas-liquid binodal. It was suggested [35] that the dynamic crossover in soft sphere fluids takes place at the line of minima of $D_T(n)$, which almost coincides with the line of minima of $D_L(n)$. This is in agreement with the previous observations for supercritical Ar [59] as well as the very first suggestions on the role of the Widom line in

the observed dynamic crossover [5]. Both quantities, thermal diffusivity and longitudinal kinematic viscosity, define the relaxation behaviour of fluids, because they define the hydrodynamic correlation times and damping of the long-wavelength collective excitations [7, 14] as well as they define the width of hydrodynamic regime [34]. It seems that namely these two quantities are responsible for the dynamic crossover for all fluids: supercritical ones and soft-sphere systems. It is necessary to stress, that the experimental studies [60, 61] were performed for fluids near the critical point. Therefore for temperatures far away from the critical region new simulation studies for Lennard-Jones fluids are required in order to check the behaviour of positive sound dispersion in a wide range of temperatures: from critical region up to very high temperatures. So far the only study [59] was performed in this direction on supercritical Ar. Its results were in agreement with the findings for soft sphere fluids [35] on the connection of thermal diffusivity D_T and kinematic viscosity D_L with the non-monotonic behaviour of positive sound dispersion. Furthermore, the NIST database [51] allows to follow the non-monotonic behaviour of the density dependence of D_T and D_L in very wide temperature and pressure ranges, that will definitely help in establishing their connection to the positive sound dispersion far away from the critical region in realistic liquids.

4.5 Conclusions

The positive sound dispersion—a viscoelastic increase of the speed of sound from the adiabatic one to its high-frequency (elastic) value—changes drastically with density and practically disappears for gas-like fluids. This was observed in IXS experiments on supercritical Ar [3, 5] and in MD simulations on many Lennard-Jones fluids. Such a change of the pressure (density) dependence of PSD was observed to take place in the supercritical fluids in the region of the Widom line being a natural extension of the gas-liquid coexistence curve. The only unclear issue of a possible separation of the liquid-like and gas-like fluids remained the case of fluids without interparticle attraction which do not have the gas-liquid coexistence and the Widom line. Recently this problem was in the focus of a molecular dynamics study [35]. That study gave evidence that the PSD behaves in the same way in soft-sphere fluids as in the Lennard-Jones ones, the crossover in PSD takes place on the line of minima of thermal diffusivity and kinematic viscosity—the fact observed for supercritical fluids too [59]. The theory of PSD, developed within the GCM approach, allowed one to connect the behaviour of PSD with the location of the Widom line in supercritical fluids above the coexistence curve. The theory is a general one—it does not depend on the particular interaction potentials. The results of [35, 59] generalize the behaviour of supercritical and soft-sphere (without the gas-liquid coexistence) fluids and extend our understanding of dynamic crossover on all types of fluids.

It is important that the vanishing positive dispersion corresponds to the density region where the thermal diffusivity D_T and kinematic viscosity D_L have their

smallest values. These two transport quantities define the damping of long-wavelength collective excitations and main hydrodynamic correlation times. Hence the results [35] for soft sphere fluids and previously for the Lennard-Jones ones [5, 34, 59] allow to conclude that the dynamic crossover between the "liquid-like" and "gas-like" states of fluids takes place similarly for fluids with and without the gas-liquid binodal in the region where thermal diffusivity and kinematic viscosity have their minima as functions of density. For supercritical fluids the correspondence between the dynamic crossover in PSD and the Widom line can be obtained by approaching the critical point [34] and using the relation between thermal diffusivity and specific heat at constant pressure.

References

1. http://www.nobelprize.org/nobel_prizes/physics/laureates/1910/waals-lecture.html
2. W. Götze, M.R. Mayr, Phys. Rev. E **61**, 587 (2000)
3. F.A. Gorelli, M. Santoro, T. Scopigno, M. Krisch, G. Ruocco, Phys. Rev. Lett. **97**, 245702 (2006)
4. F.A. Gorelli, M. Santoro, T. Scopigno, M. Krisch, T. Bryk, G. Ruocco, R. Ballerini, Appl. Phys. Lett. **94**, 074102 (2009)
5. G. Simeoni, T. Bryk, F.A. Gorelli, M. Krisch, G. Ruocco, M. Santoro, T. Scopigno, Nature Phys. **6**, 503 (2010)
6. J.R.D. Copley, S.W. Lovesey, Rep. Progr. Phys. **38**, 461 (1975)
7. J.-P. Boon, S. Yip, *Molecular Hydrodynamics* (McGraw-Hill, New York, 1980)
8. R.D. Mountain, Rev. Mod. Phys. **38**, 205 (1966)
9. C. Cohen, J.W.H. Sutherland, J.M. Deutch, Phys. Chem. Liq. **2**, 213 (1971)
10. N.H.W. Lekkerkerker, W.G. Laidlaw, Phys. Rev. A **7**, 1332 (1973)
11. A.B. Bhatia, D.E. Thornton, N.H. March, Phys. Chem. Liq. **4**, 97 (1974)
12. R.D. Mountain, Collective Excitations In Classical One-Component Liquids. *in Dynamics of solids and liquids by neutron scattering*. ed. by. Lovesey S.W. and Springer T. (Springer, Berlin, 1977)
13. L.D. Landau, E.M. Lifshitz, *Fluid Mechanics* (Pergamon Press, Oxford, 1959)
14. J.-P. Hansen, I.R. McDonald, *Theory of Simple Liquids* (Academic, London, 1986)
15. L.D. Landau, G. Placzek, Physik. Z. Sowjetunion. **5**, 172 (1934)
16. R. Zwanzig, *Nonequilibrium Statistical Mechanics* (University Press, Oxford, 2001)
17. T. Bryk, I. Mryglod, Condens. Matter Phys. **11**, 139 (2008)
18. I.M. Mryglod, V. Kuporov, Ukr. J. Phys. **55**, 1172 (2010)
19. I.M. de Schepper, E.G.D. Cohen, C. Bruin, J.C. van Rijs, W. Montfrooij, L.A. de Graaf, Phys. Rev. A **38**, 271 (1988)
20. I.M. Mryglod, I.P. Omelyan, M.V. Tokarchuk, Mol. Phys. **84**, 235 (1995)
21. I.M. Mryglod, I.P. Omelyan, Phys. Lett. A **205**, 401 (1995)
22. T. Bryk, I. Mryglod, Phys. Rev. E **64**, 032202 (2001)
23. T. Keyes, D. Kivelson, J. Chem. Phys. **54**, 1786 (1971)
24. D. Kivelson, T. Keyes, J. Chem. Phys. **57**, 4599 (1972)
25. I.M. de Schepper, P. Verkerk, A.A. van Well, L.A. de Graaf, Phys. Rev. Lett. **50**, 974 (1983)
26. S.W. Lovesey, Phys. Rev. Lett. **53**, 401 (1984)
27. T. Bryk, I. Mryglod, J. Phys. Condens. Matter **13**, 1343 (2001)
28. T. Bryk, Eur. Phys. J. Spec. Top. **196**, 65 (2011)
29. T. Bryk, I. Mryglod, J. Phys. Condens. Matter **12**, 6063 (2000)
30. T. Bryk, I. Mryglod, J. Phys. Condens. Matter **14**, L445 (2002)

31. T. Bryk, I. Mryglod, J. Phys. Condens. Matter **17**, 413 (2005)
32. T. Bryk, I. Mryglod, J. Phys. Condens. Matter **16**, L463 (2004)
33. A.Z. Akcasu, E. Daniel, Phys. Rev. A **2**, 962 (1970)
34. T. Bryk, I. Mryglod, T. Scopigno, G. Ruocco, F. Gorelli, M. Santoro, J. Chem. Phys. **133**, 024502 (2010)
35. T. Bryk, F. Gorelli, G. Ruocco, M. Santoro, T. Scopigno, Phys. Rev. E **90**, 042301 (2014)
36. T. Bryk, I. Mryglod, Phys. Rev. E **62**, 2188 (2000)
37. T. Bryk, I. Mryglod, Condens. Matter Phys. **7**, 471 (2004)
38. P. Verkerk, J. Phys. Condens. Matter **13**, 7775 (2001)
39. V. Giordano, G. Monaco, PNAS **107**, 21985 (2010)
40. Ya. Chushak, T. Bryk, A. Baumketner, G. Kahl, J. Hafner, Phys. Chem. Liq. **32**, 87 (1996)
41. T. Scopigno, U. Balucani, G. Ruocco, F. Sette, J. Phys.: Condens. Matter **12**, 8009 (2000)
42. T. Scopigno, G. Ruocco, F. Sette, Rev. Mod. Phys. **77**, 881 (2005)
43. L. Calderin, D.J. Gonzalez, L.E. Gonzalez, J.M. Lopez, J. Chem. Phys. **129**, 194506 (2008)
44. S. Sengül, D.J. Gonzalez, L.E. Gonzalez, J. Phys. Condens. Matter **21**, 115106 (2009)
45. J. Souto, M.M.G. Alemany, L.E. Gonzalez, D.J. Gonzalez, Phys. Rev. B **81**, 134201 (2010)
46. J.-F. Wax, T. Bryk, J. Phys. Condens. Matter **25**, 325104 (2013)
47. B.G. del Rio, L.E. Gonzalez, J. Phys.: Condens. Matter **26**, 465102 (2014)
48. T. Bryk, G. Ruocco, Mol. Phys. **109**, 2929 (2011)
49. D.E. Woon, Chem. Phys. Lett. **204**, 29 (1993)
50. J.-M. Bomont, J.-L. Bretonnet, T. Pfleiderer, H. Bertagnolli, J. Chem. Phys. **113**, 6815 (2000)
51. E.W. Lemmon, M.O. McLinden, D.G. Friend, Thermophysical Properties of Fluid Systems. in *NIST Chemistry WebBook, NIST Standard Reference Database 69* (National Institute of Standards and Technology, Gaithersburg MD, 2004). URL http://webbook.nist.gov
52. T. Bryk, I. Mryglod, G. Kahl, Phys. Rev. E **56**, 2903 (1997)
53. L. Calderin, L.E. Gonzalez, D.J. Gonzalez, J. Phys. Condens. Matter **25**, 065102 (2013)
54. T. Bryk, G. Ruocco, Mol. Phys. **111**, 3457 (2013)
55. T. Bryk, S. De Panfilis, F.A. Gorelli, E. Gregoryanz, M. Krisch, G. Ruocco, M. Santoro, T. Scopigno, A.P. Seitsonen, Phys. Rev. Lett. **111**, 077801 (2013)
56. K. Nishikawa, K. Kusano, A.A. Arai, T. Morita, J. Chem. Phys. **118**, 1341 (2003)
57. L.V. Woodcock, Fluid Phase Equil. **351**, 25 (2013)
58. J.L. Finney, L.V. Woodcock, J. Phys. Condens. Matt. **26**, 463102 (2013)
59. F.A. Gorelli, T. Bryk, M. Krisch, G. Ruocco, M. Santoro, T. Scopigno, Sci. Rep. **3**, 01203 (2013)
60. D.E. Wetzler, P.F. Aramendia, M.L. Japas, R. Fernandez-Prini, Int. J. Thermophys. **19**, 27 (1998)
61. J.V. Sengers, R.A. Perkins, M.L. Huber, B. Le Neindre, Int. J. Thermophys. **30**, 1453 (2009)
62. P. Jany, J. Straub, Int. J. Thermophys. **8**, 165 (1987)